MULTIAXIAL STRENGTH AND DEFORMATIONS OF CONCRETE, FAILURE MODES AND A NEW FAILURE CRITERION

Dedicated
to Dr.-Ing. Helmut Kupfer

https://doi.org/10.32970/CS.2023.1.19

Andor Windisch

The multiaxial strength of concrete, the associated stress-strain relationships, the failure modes and the failure criteria are again and again in the interest of researchers. After a historical review the most important bi- and triaxial experiments loading through brushes are analyzed. Based on the principal strengths and the loading path-concept a new, transparent type of presentation of the ultimate strength surface (USS) is introduced. For concrete classes ≤ C100 simplified relative strength-increase values are proposed. The difficulties of deformation measurements are reviewed. The outlines of future bi- and triaxial tests are discussed. Two failure modes are appointed. Stress failure criterion of biaxial state of stress are presented. Instead of the Modified Mohr-Coulomb failure criterion Extended Rankine-type failure criteria are proposed. Further systematic tests are necessary to detect the rate of participation of the loading equipment.

Keywords: Multiaxial strength, strain, ultimate strength surface, principal stresses, loading path, failure mode, failure criteria, Rankine failure criterion

1. INTRODUCTION, HISTORICAL OVERVIEW

The failure models developed until the 1960ies were defined by the testing equipment: the triaxial loading cell which was developed at the beginning of the last century by von Kármán[1]. The axial loading was performed with a solid metallic loading plate, the central-symmetric transverse loading through hydraulic pressure. Therefore, the characterization of the failure surface with the octahedral stresses without any reference to deformations was a logical consequence.

Hilsdorf (1965) proposed a brush-type loading equipment. Using brushes Kupfer (1973) carried out his well-known biaxial loading tests which made possible the characterization of concrete strength by means of the principal stresses. Ottosen (1977) applied in his model for multiaxial strength of concrete the tensor invariants. The same did CEB in its Bulletin d'Information N°. 156 (1983).

Van Mier (1984) applied brushes and proposed a triaxial representation of strength increase using principal stresses and contour lines. He emphasized that all experiments, also the uniaxial ones, are/must be essentially considered as triaxial. Based on his test data he concluded that the physical processes underlying the prepeak and postpeak stress-strain responses were basically different and should be treated separately in material models.

The fib Model Code for Concrete Structures 2010 (2013) returned to the Ottosen model and declared concrete as frictional material. "The multiaxial criteria should depend not only on shear stresses, but also on the first invariant I_1 of the stress tensor to consider the influence of the hydrostatic pressure on the ductility of the material."

As it will be shown, concrete is not a "frictional material". Especially in case of higher class concretes when the principal stresses reach the ultimate strength the concrete loses dramatically its load bearing capacity, accordingly its behavior does not allow for a treatment as a "plastic material" either. Any transformation of the non-linear stress-strain curve into a linear-elastic-"plastic" working diagram (even if with retaining the area under them) falsifies the real character of concrete.

Based on the principal stresses a new, transparent (and physically really sound) form of representation of the failure surface (USS) showing the strength increase due to bi- and triaxial loading is presented.

2. TESTS UNDER MULTIAXIAL STATES OF STRESS

2.1 Van Mier's tests

Van Mier (1984) tested specimens made of concretes with strengths between 35 and 40 N/mm² using brush-type loading equipment. His strength-envelops for bi- and triaxial experiments in the coordinate system of principal stresses (*Fig. 1*) are very transparent and informative.

Making use of the sense of these strength envelopes, the following dimensioning and control tasks can be followed (the envelopes of the relevant concrete class must be known):

– Dimensioning: in case of a given concrete class the strength $f_c^* > f_c$' shall be reached. $f_c^* > f_c$' can be achieved along the line $\sigma_1 = f_c^*$ parallel to the σ_2-axis. It must be checked what kind of constrictions perpendicular to the direction of f_c^* (i.e. σ_2/σ_1 and σ_3/σ_1) are given/possible. σ_2/σ_3 means the steepness of a line in the σ_2-σ_3 plane through the origo; σ_3/σ_1 is the coordinate of the elevation contour line of the failure surface parallel to the σ_1-σ_2 plane. The intersection of

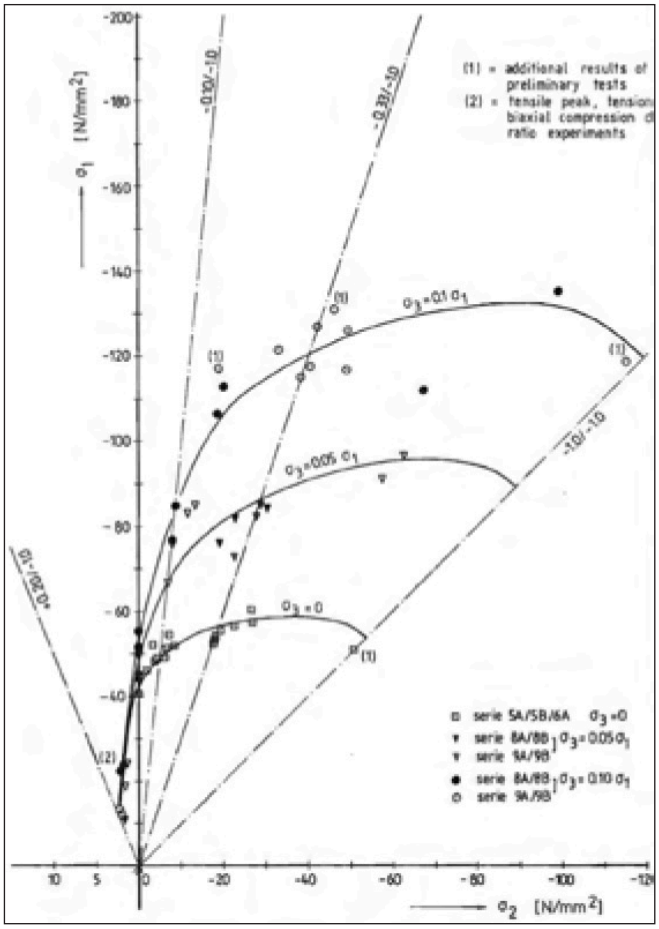

Fig. 1: *Strength-envelopes for the bi- and triaxial experiments of van Mier (1984). (The tensile axis σ_2 is drawn at a larger scale!) Authorized reprint of Fig. 5.8 of a PhD thesis elaborated at TU Eindhoven.*

the $\sigma_1 = f_c^*$ –line with the line with the steepness of σ_2/σ_3 in relation to the next two σ_3/σ_1-contours along the σ_2/σ_3-line gives the necessary rate of confinement in the direction of σ_3. (Note: the numbering of the principal axis is acc. to van Mier, it differs from that used later in this paper.)

– Control: concrete class, σ_1/σ_3 and σ_2/σ_3 are given. The position of the point along the σ_2/σ_3-line corresponding to the σ_1/σ_3-ratio shall be determined. The σ_3 ordinate of the intersection is the achievable strength, f_c^*. If $\sigma_3 \geq f_c^*$ then the strength criterion is fulfilled, otherwise
  - o either the rate/s of confinement shall be changed or
  - o a higher concrete class shall be chosen.

As in the tests

– the most possible endeavor was made to have the principal axis parallel with the sides of the cubic specimens,
– as the principal components are the most fundamental characteristics of any state of stress
– as concrete (and the specimens, too) are never isotropic (at least the direction of compaction has some significant impacts)

hence any transition to the invariants of the deviatoric stress tensor is rather meaningless.

An important statement of van Mier is: “From the statistical analysis of both, the bi- and triaxial series no effect of cyclic or monotonic loading on the envelope curve was observed. The stress-strain curves for concrete seem to be unique, and all stress- and strain conditions within the envelope-curve may exist.”

The Author means that whereas the minor compressive- or maximum tensile principal stress is the ‘basic’ influencing factor for the size of the failure strength, the intermediate principal stress is the more important variable. This can be easily realized: in case of the biaxial compression test the ‘basic’ factor is σ_1=0. The size of the intermediate stress σ_{2u} defines the size of σ_{3u}! In case of a constant $\sigma_1 > 0$ principal stress the size of σ_2 governs σ_3. Two comments:

- All failure models ignoring the direct reference to intermediate principal stress must fail. This means that neither the Mohr- nor the Coulomb-failure criteria or any of their modifications can be applied for the proper characterization of concrete.
- Models based on the invariants do not allow for a clear understanding of the impact of the intermediate principal stress.

Van Mier reported that the direction of the loading with regard to the direction of casting had a significant influence on strength and deformational response of the specimens. This doubts further whether the description of the failure surface using the tensor invariants could be correct?

Due to its normal method of manufacture (pouring and compaction) concrete is not isotropic.

The role of the highest (i.e. smallest compressive) principal stresses in triaxial compression tests is similar as specified for σ_2 in the biaxial tests.

2.2 Tests of Speck

Speck (2007) carried out bi- and triaxial loading tests in compression using brush-type loading equipment. She tested 100 mm cubes made of high and ultrahigh strength concretes, also with fibers. In this paper her results with BI (f_c’=56 N/mm²), BII (f_c’=85 N/mm²) and BIII (f_c’=93 N/mm²) concretes without fibers will be considered. The specimens in the triaxial tests for uniaxial compressive strength were loaded parallel to the direction of pouring/compaction whereas in the biaxial tests perpendicular to it. Speck found a pronounced influence of the direction of compaction on the uniaxial compressive strength: parallel loaded the strength was ~10% higher than loaded in transverse direction. Nevertheless the data do not confirm this. Van Mier (1984) did not observe a similar effect.

Speck developed an Ottosen-type failure criteria with improvements related to the brittleness of the UHPCs (this will not be treated here).

2.3 Tests of Ritter

For testing UHPC specimens containing fibers primarily in tension-compression-compression loadings in the triaxial loading equipment at TU Dresden Ritter (2014) developed a new type of tensile load transmission.

3. NEW TYPE OF PRESENTATION OF ULTIMATE STRENGTH SURFACE

3.1 Fundamentals

The most important basic statement: All experiments, also the uniaxial ones must be essentially considered as triaxial.

Concrete obeys principal stresses only. Concrete does not have any shear strength. Shear stress is the consequence of our hugging to the global coordinate system only.

All possible combinations of stresses which correspond to an ultimate stress state can be expressed in terms of principal

stresses normalized to the uniaxial compressive strength as an Ultimate Strength Surface (USS).

The stress state in a point is characterized with the three principal strength values and the direction of the principal axes. The stresses are ordered as follows: $\sigma_1 \geq \sigma_2 \geq \sigma_3$. Compressive stresses and strains are negative, the tensile ones are positive. (The uniaxial compressive strength is considered as a positive value.)

The following notations are introduced:

- σ_1 and σ_2 are related to σ_3, accordingly $\sigma_{1u} = \gamma\ \sigma_{3u}$ and $\sigma_{2u} = \lambda\ \sigma_{3u}$.
- The loading occurs along a "loading path", i.e. during loading the ratios γ and λ remain constant, the triade [γ, λ, 1] characterizes a stress-loading path. (Note: plastic theory is valid in case of one-parametric loading only!)
- σ_{3u} is the most negative strength at failure along any stress-loading path
- The invariants of the stress and of the strain tensors remain – as non-transparent and misleading quantities – ignored. Accordingly the hydrostatic axis, the deviatoric plane, the requirement for the (not realistic) three-fold symmetry and the convexity of the polar figures disappear, too.
- The hydrostatic stress and strain and the octahedral shear stress and strain, which hinder the direct examination of the impact of the three (maximum, intermediate and minimum) principal stresses and strains on the failure surface, disappear.
- Notions as "equibiaxial" and "equitriaxial" tensile strengths disappear as well: in an equibiaxial tensile test the tensile failure will occur according to the actual direction-dependent scatter of the tensile strength, independent of each other in the two other directions. The same is valid for the equitriaxial tensile tests. The reason is, that –in contrary to the compressive loading, where in transverse direction to the compressive stresses micro- and later discrete macro-cracks occur which influence the actual strength there- the tensile failure occurs in a 'thin' region only perpendicular to the direction of tensile force hence does not influence the tensile strength in the two other directions (See Fictitious Crack Model of Hillerborg et al. (1976)).
- The results of the bi- and triaxial tests (σ_{3u}) will be displayed in the coordinate system γ, λ as $\sigma_{3u} = \Phi\ (\gamma, \lambda)$. Advantages of this display are:
  - The direct impact of the minimum and medium principal stresses, resp. can be perceived,
  - USS is a continuous, smooth, convex, single-valued surface,
  - As $\gamma \leq 1$, $\lambda \leq 1$ hence USS is always limited, no extra "cap function" as in case of the octahedral strength function is needed.
  - The $-\sigma_{3u}/f_c'$ values along the [0, 0] to [1, 1] diagonal correspond to the "compressive meridian", whereas along the [0, 1] to [1, 1] line correspond to the "tensile meridian".
  - If the pouring direction coincides with the $-\sigma_{3u}/f_c'$-axis then the $-\sigma_{3u}/f_c'$-surface is axisymmetric to the [0, 0] – [1, 1]-diagonal.

It should be recognized that for each concrete class only two failure configurations characterized with the triade [γ, λ, 1] exist: i) the direction of σ_{3u} coincides with the direction of the pouring/compaction, ii) it does not coincide. This means that each failure surface displayed in the (σ_1, σ_2, σ_3) coordinate system is single-valued over the (σ_1, σ_2)- or (γ, λ)-planes.

The description using the octahedral stress components suggests an axis-invariance which in the case of concrete (if only because of the direction set by the compaction) might lead to faulty assumptions as due to its production technology concrete is not isotropic.

In case of three dimensional representations (relative increase of strength) the two horizontal axis correspond to the γ and λ values and the vertical one to the $\Phi = -\sigma_{3u} / f_c'$-values.

The renunciation from the hydrostatic- and deviator-related representation yields a

i. clear and transparent understanding of the influence of the minor (γ)- and intermediate- (λ) stress levels resp.,
ii. deviating from the compulsory three-fold symmetry with respect to the hydrostatic axis the figures meet the non-isotropic characteristics of the concrete which is the direct consequence of concrete production technology (pouring). It is even more pronounced in case of the fiber-reinforced and printed concretes which are more and more coming.

3.2 Ultimate strengths in triaxial state of stress

Van Mier's (1984) test results in the proposed form of representation can be seen in *Fig. 2*. With increasing γ the $-\sigma_{3u}/f_c'$ values increase whereas in case of $\lambda = 1$ the $-\sigma_{3u}/f_c'$ values are less than in case of $\lambda = 0.6$.

Fig. 3 shows a level-type representation of relative strength-increase measured by Speck (2007) at her BII concrete.

Fig. 2: *Van Mier's tri-axial test results in the new form of representation*

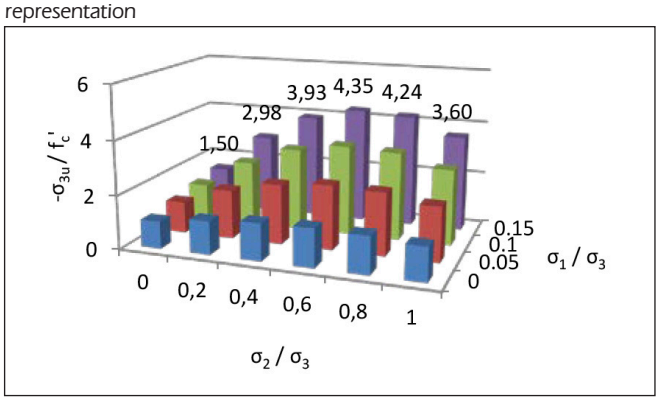

Fig. 3: *Level-type representation of 3D strength of Speck's BII (f_c' = 71 N/mm²) concrete: a) the whole tested field, b) the symmetrical region $\gamma \leq 0.15$, $\lambda \leq 0.15$*

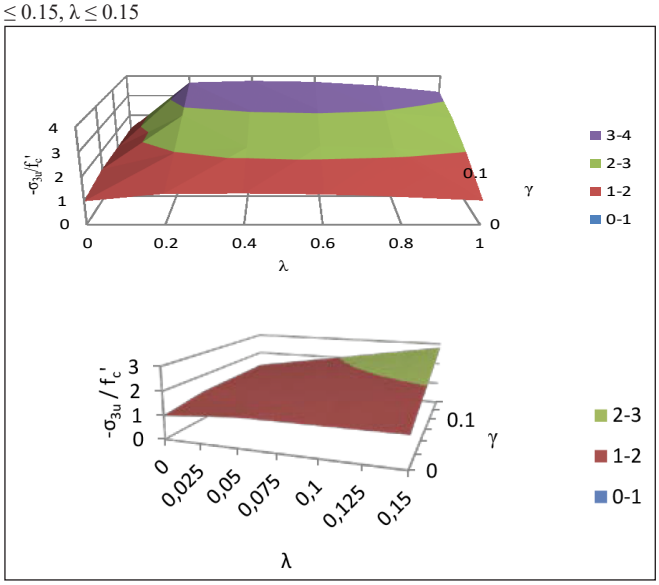

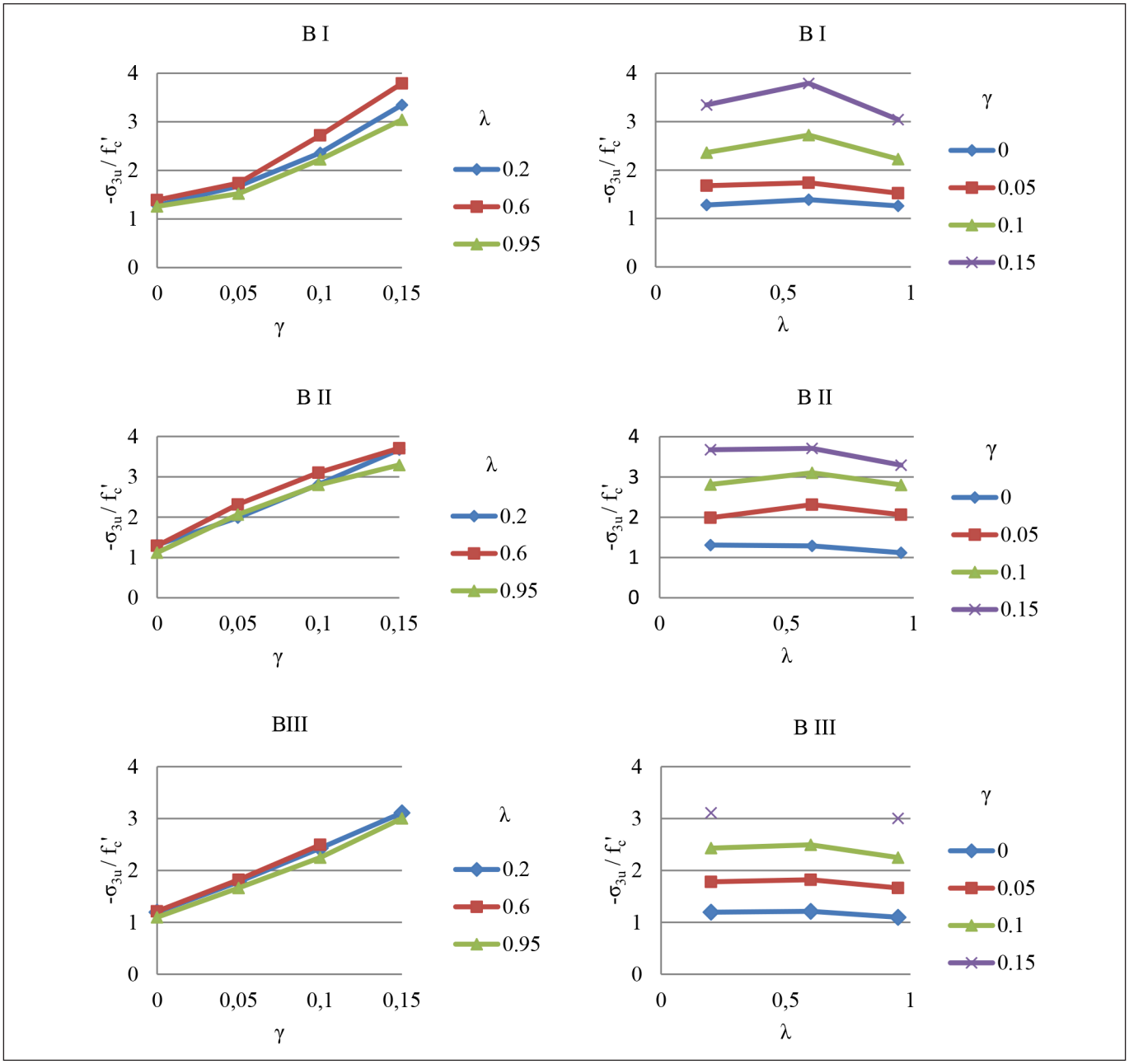

Fig. 4: Segments of the USS for concretes tri-axially tested by Speck for a) λ = const, b) γ = const.

Fig. 4a) and b) show the sections along the λ = const. and γ = const. lines of the 3D ultimate strength surfaces for concretes tested by Speck. The courses in *Fig. 4a*) imply that –at least within the tested region 0 ≤ γ ≤ 0.15– no tendency for a downward, slowing growth of the normalized strength increase can be detected.

Fig. 5 shows the relative strength increase of the three concretes tested by Speck (2007) for the three λ-values as function of γ. As a matter of fact the differences between the courses of the relative strength-increases for the three concrete classes along the λ = const. lines are within the possible scatters of the tests, no characteristic differences can be detected. Even the order of the increasing concrete strengths cannot be discerned. This can be interpreted that at least in case of concrete classes < C100 generally valid -σ_{3u}/f_c' values as linear function of γ can be defined hence no further test-series are needed. At γ = 0.15 -σ_{3u}/f_c'-values could be 3.5 (for λ = 0.2), 3.7 (for λ = 0.6) and 3.3 (for λ = 0.95). The sections along the λ=const. lines up to the tested γ ≤ 0.15 ratio do not yield enough information for estimation of a convex course or even a limit value of the hydrostatic compressive strength of these concretes. *Fig. 2 to 5* reveal the advantages of the proposed new type of presentation.

4. PROBLEMS AND DIFFICULTIES AT DEFORMATION MEASUREMENTS

Deformation measurement is complicated when brush-type bearing platens are used. Four or all six surfaces of the specimen are "occupied" with the brushes. On the free surface DMS or optical sensors can be applied. Here the limited sensor length might cause a problem: the failure procedure occurs through development of discrete cracks from microcracks. If the discrete crack occurs outside the sensor length, then the measured deformation is not characteristic. The transversal deformation perpendicular to the free specimen surfaces can be measured mechanically in a discrete point (Kupfer (1973) has chosen two points in 4 cm distance from the corners of the 20*20 cm² specimen). Here once more the question arises whether the deformation in this point is typical for the whole

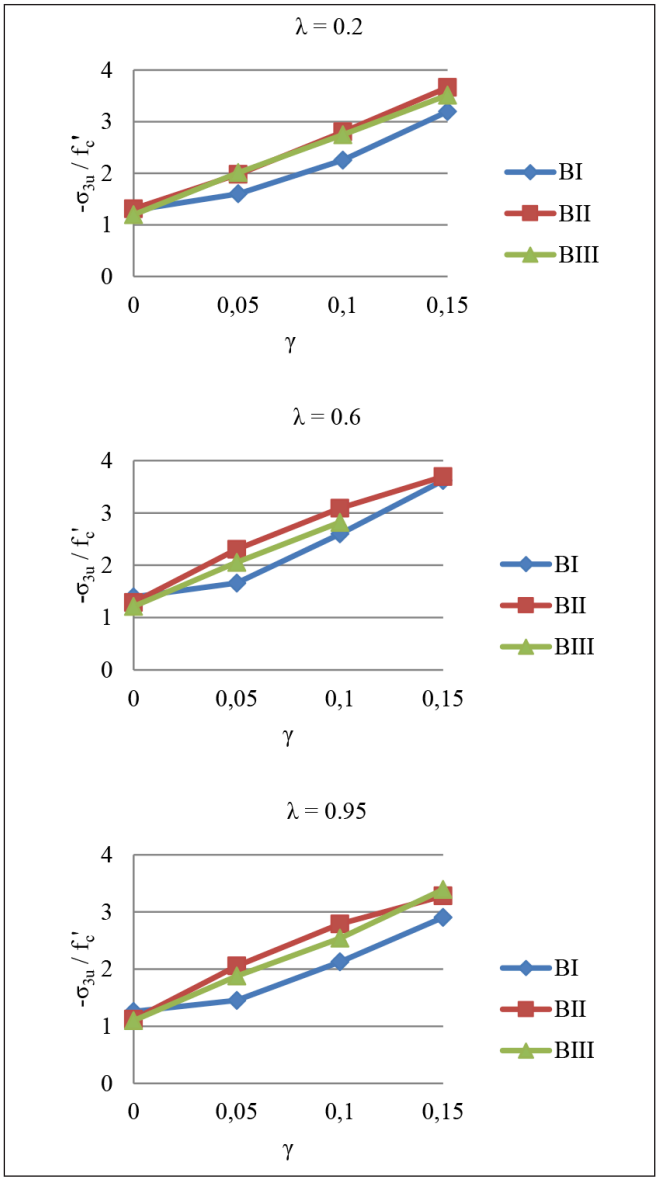

Fig. 5: Normalized ultimate strength increase of the three classes of concrete tested by Speck[8]

specimen? Measuring elements can be put into the specimen: Ritter (2014) applied tetrahedron shaped wire-scaffolds mounted with optical sensors. Here the gauge or its carrier causes discontinuity in the specimen influencing its behavior. Another possibility is to measure the deformations between two elements of the brush (van Mier (1984), Speck (2007)). Here the question arises whether the brush correctly follows the deformation of the specimen's surface (eventual slip).

The strain values published by Speck (2007) are mean values of up to six measurements (which were made with the greatest possible care). Nevertheless, mean values may sometimes deform/obscure the real physical relationships. Speck reports in detail on the problems that were arisen from the additional forces caused by the flexural rigidity of the brush-teeth. This measuring method cannot detect discrete cracks which develop during the loading procedure.

The conclusion of van Mier (1984) is pointing the way: the results are well within the 'engineering accuracy' (but not more). He reports that the outer parts of the cubic specimens behaved/deformed in a different way as the central parts: the deformation of the brush-rods and the specimen results in a spherical loading surface. Van Mier mentions that cracks developed in the descending branch of the stress-strain curve, which is important for the evaluation of the deformations.

5. ULTIMATE STRAINS IN MULTIAXIAL TESTS

Fig. 6 shows the courses of the mean values of the measured failure strains in the biaxial tests ($\gamma = 0$, compression-compression sector) of normal concretes measured by Kupfer (1973) (f_c' = 19 N/mm², 32 N/mm²), high strength concretes tested by Speck (2007) BI (f_c'=56 N/mm²), BII (f_c'=85 N/mm²) and BIII (f_c'=93 N/mm²) and Ultra High Performance concrete by Ritter (2014) (f_c' = 171 N/mm²) as function of λ.

The following general observations can be made for each concrete class:

- the ε_{3u} strains (in the direction of the major compressive stress) remain around -3‰ as λ increases
- the ε_{2u} strains (direction of the intermediate stress) decrease continuously linearly (from positive to negative parallel with the increasing, relative compressive loading in direction 2) unless they arrive at the same value as in the minimum strength direction (with scatter).
- the tensile strain ε_{1u} (deformation in the unloaded transverse direction) continuously increases with the increasing relative compressive loading in direction 2, the elongation exceeds very soon the strain limit assigned to the very limited uniaxial tensile strength of concrete. The measured elongations cannot detect the discrete cracks,
  - the max. value of ε_{3u} is not less than -4‰, nevertheless, no real trend between concrete strength and deformation can be detected, this means that the deformation in the most loaded direction cannot be considered as singular failure criterion,
  - beyond that the tensile strains, ε_{1u}, increase with increasing λ, no regularity can be detected either,
  - for simplicity reasons at the development of the stress-strain curves at different λ-values a linearity between the relevant ε-values measured under the uniaxial- and the biaxial loading can be considered.

Fig. 7 shows the ε_{1u} and ε_{3u} strains for BII concrete as function of γ, measured in triaxial tests, published by Speck (2007). It is conspicuous that the ε_{1u}-value for $\gamma = 0$ is not compatible with the following values for $\gamma > 0$ values. The range of the tested γ-values does not allow any sensible extrapolation for the further course of the strains.

The following trends can be diagnosed:

- ε_{1u} increases far beyond the strain related to the uniaxial tensile strength (in case of $\gamma = 0.05$ up to 2.49 ‰, of $\gamma = 0.10$ up to 4.72 ‰, and of $\gamma = 0.15$ up to 6.11 ‰). This means that not negligible compressive stresses ($\lambda\sigma_{3u}$) must be transferred despite/across the numerous macrocracks. Here the large-scale influence of the loading equipment (its lateral stiffness) shall be investigated in the future.
- ε_{3u} continuously increases (i.e. shortening decreases), at the same time (in case of $\gamma = 0.05$ from ~ -2 ‰ up to -1.75 / -1.6 ‰, of $\gamma = 0.10$ from -4.73 ‰ up to -4.23 ‰, and of $\gamma = 0.15$ from -8.28 up to -5.12 ‰).

The course of the maximum strains in direction of the lowest (ε_{1u}) and of the highest (ε_{3u}) compressive stresses, resp. as function of λ (at $\gamma = 0.05$) for a wide range of concrete classes, presented in *Fig. 8*, shows that both deformations have a decreasing tendency at increasing concrete strengths.

At all observations and conclusions the normal scatter due to the very different concrete compositions, strain measuring methods etc. must be considered.

The experimental studies have shown that the deformation

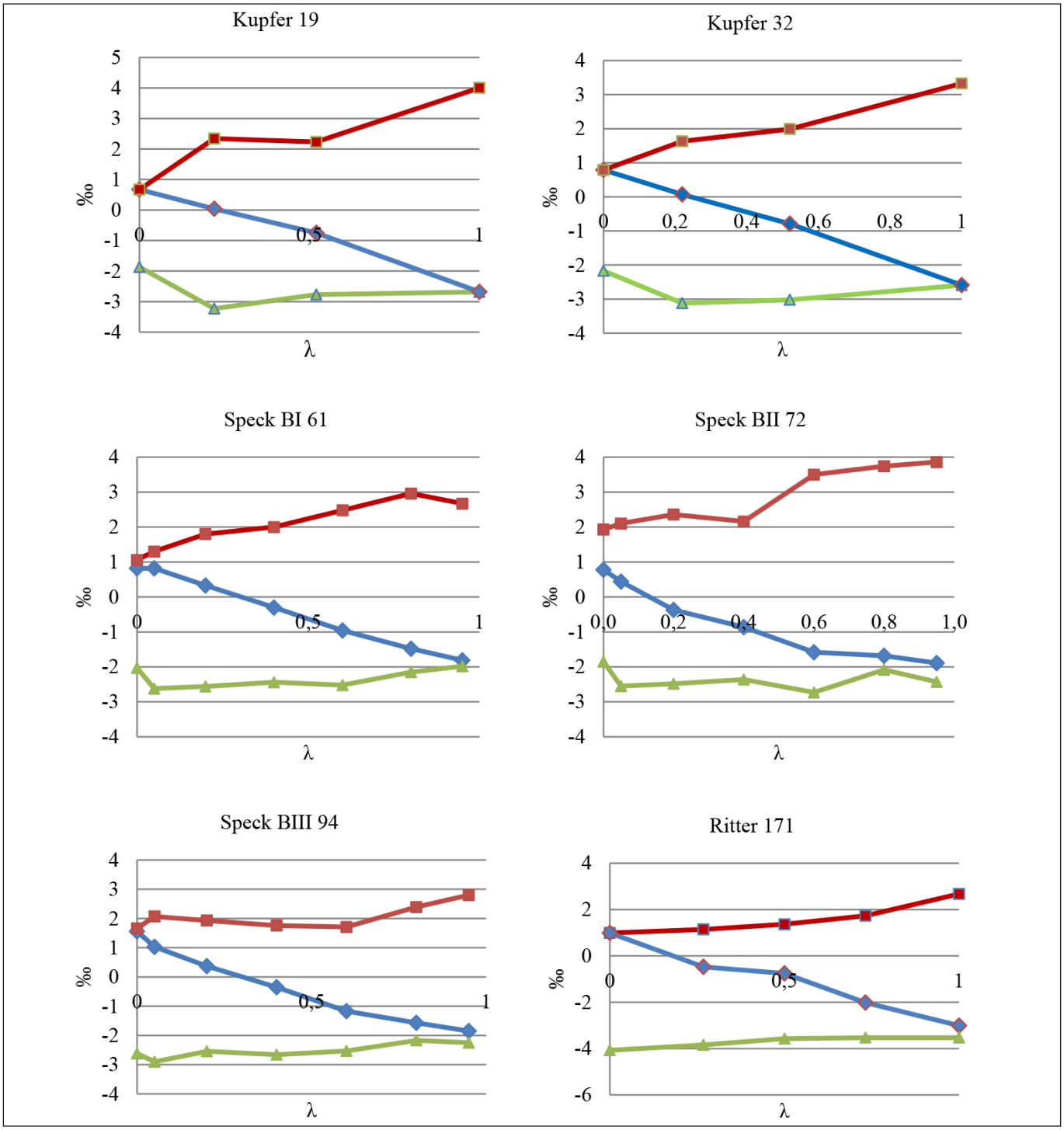

Fig. 6: Ultimate strains measured in biaxial tests Legend: red – ε_{1u}, blue – ε_{2u}, green – ε_{3u}

characteristics and the ultimate strength of concrete subjected to uni-, bi- or triaxial stresses are controlled by the development and propagation of microcracks. These microcracks are mainly oriented in a perpendicular direction to the direction of the smallest principal compressive stress or the largest principal tensile stress. (It is one more reason to leave the octahedral stress-type representation.)

6. FUTURE OF 3D-TESTS

The history of bi- and triaxial tests with HPC- and UHPC-specimens reveals that the capacity of the loading brushes restricts the applicable γ- and λ-ranges. *Fig. 9* gives useful information: as higher is the concrete strength, as lower is the relative strength increase. Similar tendency can be detected in *Figure 10*: the relative triaxial strength increases measured

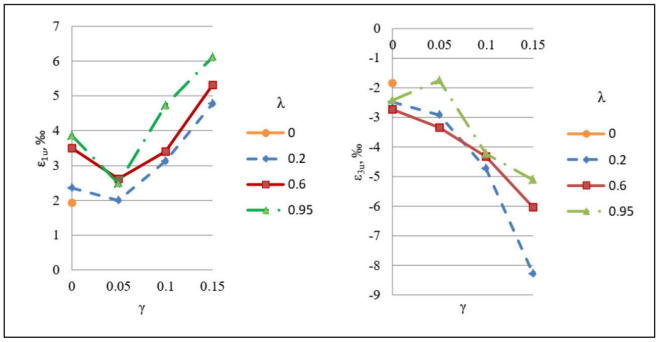

Fig. 7: Development of the strains a) ε_{1u} and b) ε_{3u} under tri-axial loading of BII specimens, measured by Speck

at γ = 0.027 (very low) and different λ-values for Ultra High Strength concrete (Ritter (2014)) are regularly smaller than those in case of High Strength concretes (Speck (2007)).

This means that using an existing (brush-type) loading

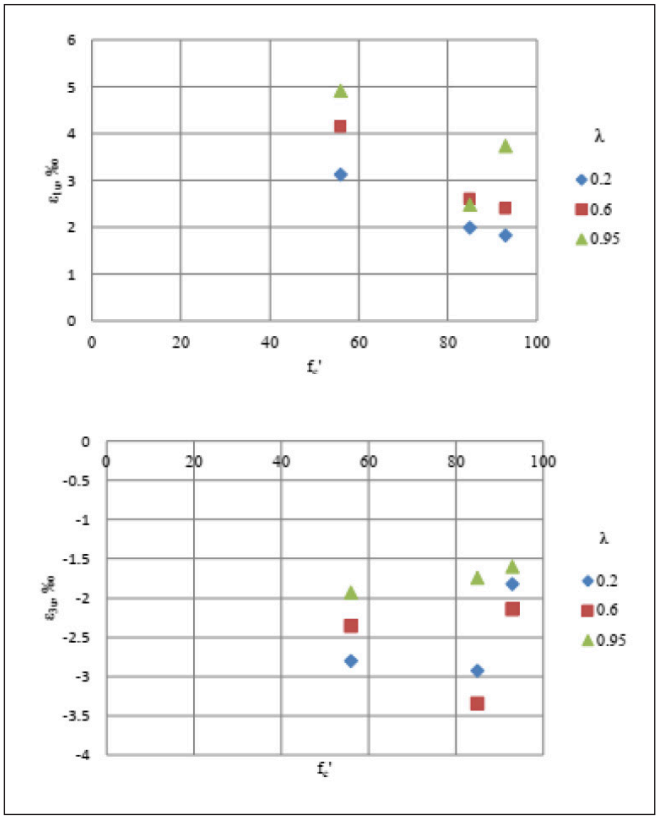

Fig. 8: Courses of strains ε_{1u} and ε_{3u} as function of the uniaxial concrete strength at $\gamma = 0.05$

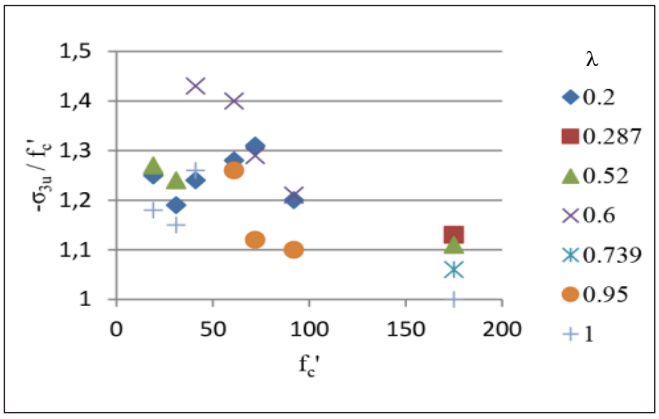

Fig. 9: Relative increase of relative ultimate biaxial compressive strength of different concrete classes (f_c' = ~40 – 175 N/mm²) as function of λ

equipment with given load bearing capacity and following a [$\gamma > 0.15$; λ; σ_{c3u}] (or similar) loading path, specimens with increasing compressive strengths should be loaded up to failure. The smallest value of the measured $-\sigma_{c3u}/f_c$'-values yields an upper limit of the possible $--\sigma_{c3u}/f_c$'-values for all higher strength concretes.

Certainly the impact of the rigidity of the loading brushes should be systematically investigated and taken into account.

7. FAILURE MODES

In the literature five failure modes are listed:

1. tensile failure: main crack perpendicular to highest principal stress
2. compression failure: the specimen fails to columns parallel with the highest compressive stress
3. splitting failure: the specimen fails to slices perpendicular to the smallest compression stress
4. shear failure: with inclined failure surfaces, where only a limited number of cracks develop, which are approximately parallel with the medium principal stress and perform an angle approx. 20-30° to the smallest principal stress
5. crushing failure: the internal structure of concrete is destroyed, the pores fail, many cracks without orientation develop.

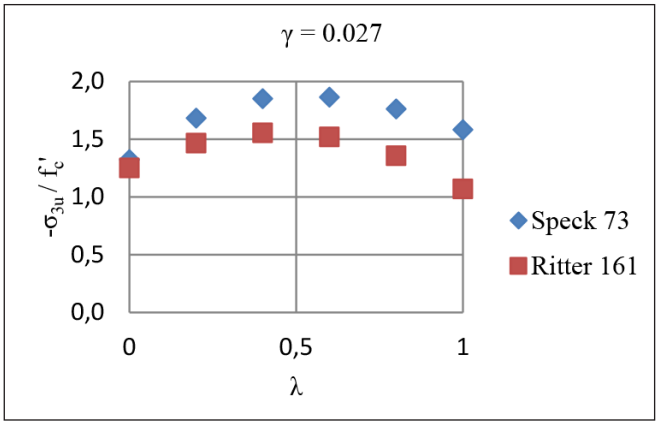

Fig. 10: Comparison of relative increase of tri-axial strengths of High and Ultra High Strength Concretes

Comparing the modes 1-3 it can be realized that in each of these modes the tensile deformation capacity was exhausted. Referring to failure mode 4 we recall to van Mier's (1984) hints: "According to investigations carried out by Newman et al. (1965), this "shear-plane" fracture mode should be attributed to a non-uniform stress-distribution within the concrete. This is the result of a rotation of one of the loading plates, when an experiment is carried out with one end effectively fixed and the other end effectively pinned. The effect may even become more significant when non-homogeneous specimen is tested." In van Mier's investigation the prisms were loaded perpendicular to the direction of pouring, which implies that one side of the prism could be weaker. The specimen's neutral axis did not coincide with the loading axis. The prisms failed with cracks running more or less parallel to the direction of loading. "The difference in fracture mode of specimen did not seem to influence the macroscopic stress-strain curve. Probably the rotation of the upper loading platen is reflected by unevenness in the descending branch and the effect is not pronounced when perpendicular loading (i.e. to the direction of pouring) is applied." Conclusion: failure mode 4 (if it occurs) is an anomaly. This conclusion can be confirmed with reference to the contradiction between the geometrical boundary conditions (plane end of the loading brush and support plate) and the relative displacements necessary for the development of the wedges corresponding to the shear failure (wedges must undergo a mutual shifting) these are not compatible with each other.

Failure mode 5 is used by the cement chemists to squeeze pore water from very small concrete probes, i.e. it is not relevant for structural engineers.

The 'hugging' to the shear stress oriented failure criterions like Mohr-Coulomb can be understood/excused as due to the axial loading through the rigid steel plates (friction) and the dumpy test specimens ($h/d \leq 2$): in all cases the failure patterns showed inclined 'shear' failure planes, similar to those at uniaxial compressive tests on cubes and dumpy cylinders.

All 'shear band ruptures' must be regarded as reminiscences and tribute to the aforementioned inclined shear failure planes seen in former imperfect tests. Van Mier (1984) reports that some of the shear-band type failures were caused through the spherical deformation of the loading brush: Shear

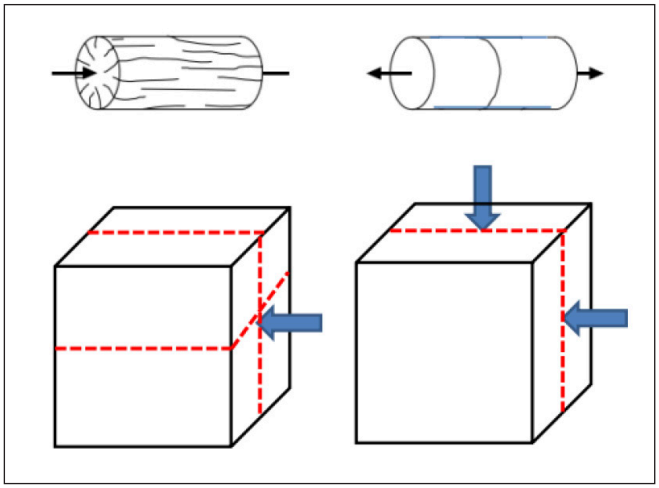

Fig. 11: *Macrocracks (schematic representation) in specimens loaded in a) cylinder in uniaxial compression, b) uniaxial tension, c) cubes in uni- and biaxial compression*

plane fracture was observed for four of the eight prism tests. This means, that in four of eight cases neither the loading brush deformed nor the specimen performed "prefabricated" weak planes: the four shear plane fractures are the "abnormal" ones.

The 'cone-like' rupture elements are formed when a shear-band develops through an array of initial parallel tensile micro-cracks. This tensile crack-array was visualized by Stroeven (1973) using the fluorescenting technique.

In fact two fracture patterns for concrete with only one single inherent cause exist: microcracks occur in plane(s) parallel with the major compressive load or perpendicular to the maximum tensile load. In the section with the weakest tensile strength microcracks form a macrocrack (*Fig. 11*). In case of compressive loading the parts formed by the cracks might continue to carry the compressive loading, whereas in case of tension the first crack stops the loading procedure, unless the stiffness of the loading brushes takes over some tensile stresses.

Similar fracture pattern was observed in high-performance concrete for all tested stress ratios and all concrete classes by Speck (2007). Crack formed, which run parallel to the unloaded surface. In the uniaxial tests and partly under the stress ratio $\lambda = 0.05$, cracks appeared in two planes, parallel to the unloaded surfaces and parallel to the slightly loaded surface. For all other biaxial stress conditions, there was the crack plane quite parallel to the free surface. The specimen was split into several slices. The parallelism of the crack planes with regard to the unloaded surface increased beyond $\lambda = 0.6$ in the second load axis and with increasing concrete class.

An interesting issue should be mentioned: the authors of the different fracture criteria operating with meridians argue over the shape of the meridians and their closure resp. at high hydrostatic loading, i.e. on the size of the 'cap' value. Considering the possible failure modes in case of the loading path $[1, 1, \sigma_{c3u}]$ we must conclude that only a full crushing of the concrete texture can occur as the concrete chemists squeeze the pore water for their investigations. A 'cap' strength value is difficult to assign.

8. FAILURE CRITERIA

Three types of criteria could be considered:

- Strength(s) or their combination at failure
- Strain(s) or their combination at failure
- a combination of both.

With regard to strength, reference is made to Section 3.2.

What about the strain(s)? Figure 7a shows the development of the ε_{1u} strains (elongation) as function of γ, measured in the triaxial loading tests (compression-compression sector) of Speck (2007). It is conspicuous that despite of the considerable elongations, compressive stresses up to 45 N/mm² can/must be transmitted in this direction. This must be understood as "contribution" of the loading system, and makes any statement about a failure criterion rather questionable.

Van Mier (1984) diagnosed: "The tests show clearly the interaction between stress- and deformation." "It seems more appropriate to describe the specimen response as 'structural' rather than as 'material property'."

Due to the problems and difficulties at deformation measurements (as discussed in chapter 4) no reliable failure criteria referring to strains can be defined.

As a conclusion it must be discovered, that due to the unknown degree of participation of the different loading brushes, for the time being neither the measured strengths nor the published strains are correct characteristics of the failure of the tested concretes.

In order to quantify the rate of participation of the loading equipment further systematic tests are necessary: following identical and characteristic loading paths specimens of the same concrete strength must be tested with significantly different stiff loading brushes!

Thereafter it can be tried to formulate a reliable failure criteria for multiaxially loaded concrete.

8.1 Ottosen's Model

Ottosen (1977) lists as advantage of the description of his failure criterion (surface) as function of the invariants: (1) only four parameters are used; (2) makes determination of the principal stresses unnecessary; (3) the surface is smooth and convex with the exception of the vertex; (4) the meridians are parabolic and open in the direction of the negative hydrostatic axis; (5) the trace in the deviatoric plane changes from nearly triangular to circular shape with increasing hydrostatic pressure; (6) it contains several earlier proposed criteria as special cases, in particular, the criterion of Drucker and Prager (1952) and of van Mises.

The four parameters can be determined with tedious calculations from the uniaxial tensile strength, uniaxial compressive strength, equibiaxial compressive strength and an ultimate strength on the compressive meridian. Advantage (2) does not exist: the invariants are composed from the principal stresses nevertheless the invariants make the failure criterion extremely non-transparent. The influence of the distinct principal stresses and trace the load path cannot be perceived.

8.2 CEB Bulletin No. 156

In the CEB Bulletin No. 156 (1983) the description of "the Ultimate Strength Surface (USS) is based on the following technical considerations and rational reasoning:

a. USS is to be described by invariants of the stress tensors or by expressions derived from it
b. For an isotropic material without any history, the USS in the deviatoric plane (polar figure) is three-fold symmetric with respect to the hydrostatic axis.
c. Theory of plasticity and more recent fracture mechanics

studies require the polar figures to be convex.

d. For a material whose uniaxial compressive strength differs from its tensile strength we have to distinguish between a triaxial compression curve and a triaxial tension curve."

Comments

To a): already Kármán (1910) wrote in 1910: "If the principal stresses are considered as spatial coordinates then each point in the space corresponds to a certain state of stress. The points corresponding to the limit of elasticity form a surface, which encloses that portion of space where purely elastic deformations occur. This surface is called limit surface of elasticity. Another surface corresponds to the maximum stress states which act just before failure occurs." As it is well known, the sense of invariants of a tensor (here the stress tensor) is that it does not change with rotation of the coordinate system. (But this is its single sense.) The description of USS by invariants makes the stress state non-transparent and less practical. Much better is to transfer any stress state into its principal stresses with the corresponding directions. Concrete "perceives" principal stresses only. The description by hydrostatic normal and octagonal shear stress was essential as at the early experiments in the triaxial cells only the longitudinal principal stress was explicit; all perpendicular directions were "principal" directions. The octagonal stress components "helped" to overcome this 'inconvenience'.

To b): due to its production technology (pouring), concrete is not isotropic. In the era of the high capacity computers there is no reason to adhere to this not existing isotropy.

To c): recent test series (van Mier (1984), Speck (2007)) revealed that -especially in case of concretes beyond C40- the upper bound theory of plasticity cannot be applied to concrete. The "plasticity" of RC slabs results from the "residual elasticity" of the concrete compression zone of slightly reinforced cross sections. This plasticity attributed to the concrete compression zone "results" of the difference between the depth of compression zone calculated assuming perfect bond between rebars and concrete, and the real behavior of the cracked RC section, provided that low amount, moderate diameter rebars are applied.

To d): the triaxial compression curve (or meridian) and the triaxial tension curve are direct "results" of the physical possibilities of the ancient triaxial cells: the stresses in the transversal directions were always identical, which corresponds to the definition of these meridians. In a description of the USS in the coordinate system of principal stresses these meridians are meaningless.

8.3 MC2010

Among several acceptable formulations MC2010 (2013) has chosen the constitutive equation of Ottosen (1977) as "it is not too difficult to use and agrees well with test data".

The mean value of strength under multiaxial states of stress may be estimated from the failure criterion

$$\alpha \frac{J_2}{f_{cm}^2} + \lambda \frac{\sqrt{J_2}}{f_{cm}} + \beta \frac{I_1}{f_{cm}} - 1 = 0$$

where

$$\lambda = c_1 \cdot \cos\left[\frac{1}{3} \cdot arccos(c_2 \cdot cos3\theta)\right]$$

$$\cos 3\theta = \frac{3\sqrt{3}}{2} \cdot \frac{J_3}{J_2^{3/2}}$$

The material parameters α, β, c_1 and c_2 depend on the uniaxial compressive strength f_{cm}, the uniaxial tensile strength f_{ctm}, the biaxial compressive strength f_{c2cm} and the triaxial compressive strength at one point of the compressive meridian ($\sigma_1 = \sigma_2 > \sigma_3$) described by σ_{com} and τ_{com}. In order to determine these coefficients five additional parameters have to be calculated. It must be diagnosed that the Ottosen model is not transparent.

8.4 Multiaxial states of stress: recommendations in MC2010

MC2010 (2013) writes: "Basically, yield functions *f* can be chosen based on multiaxial failure criteria for concrete. These criteria should depend not only on shear stresses, but also on the first invariant I_1 of the stress tensor to consider the influence of the hydrostatic pressure on the ductility of the materials. Thus, formulations as

- the Rankine criterion, where tensile failure occurs when the maximum principal stress reaches the uniaxial tensile strength,
- Drucker-Prager criterion, which is modification of von Mises criterion including the influence of hydrostatic pressure on yielding,
- Mohr-Coulomb criterion, where the maximum shear stress is the decisive measure of yielding, and the critical shear stress value depends on hydrostatic pressure, and
- modifications or combinations of them

can be used in concrete plasticity models. Concrete is a frictional material."

Some comments:

- Rankine criterion is valid not only in tension-tension sector but in all other sectors, too. Extended Rankine-type failure criteria for concrete was proposed recently by the Author (2022).
- Mohr's model does not consider the influence of the intermediate principal stress.
- Concrete is not a frictional material. The failure in compression, too, occurs in form of discrete tensile cracks, relative displacements which could induce friction stresses do not occur at all, or at a 'late' stage of the load- and deformation state only where the crack widths are already so large that only very limited frictional stresses can occur.

Here elementary further research is still needed!

9. STRESS FAILURE CRITERION FOR BIAXIAL STATE OF STRESS

9.1 Ratio of Compressive to Tensile Strength

In MC2010 (2013) the mean value of uniaxial tensile strength f_{ctm} in [MPa] is defined as

$$f_{ctm} = 0.3\,(f_{ck})^{2/3} \quad \text{for concrete grades} \le C50 \qquad (1)$$

$$f_{ctm} = 2.12 \cdot \ln(1 + 0.1 \cdot (f_{ck} + 8)) \quad \text{for concrete grades} > C50. \qquad (2)$$

Windisch (2021) defined the ratio

$$\chi = f_{ck}/f_{ctm} \qquad (3)$$

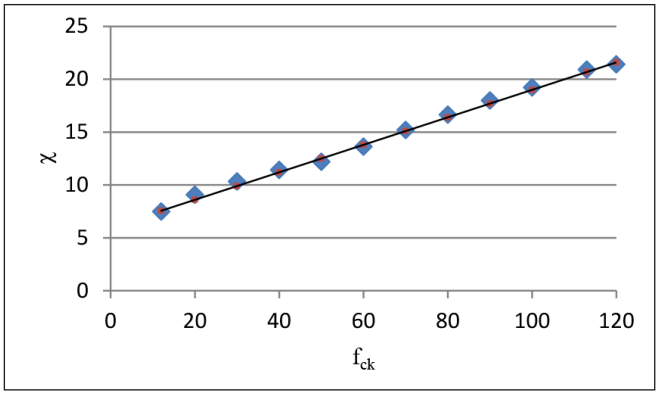

Fig. 12: Ratio of compression strength to tensile strength (χ) as function of f_{ck}

i.e. the mean value of uniaxial tensile strength f_{ctm} as function of the characteristic compressive strength, f_{ck} (*Fig. 12*).

Fig. 12 reveals that the simple linear function

$$\chi = 0.13\ f_{ck} + 6 \qquad (4)$$

describes quite exactly the interrelation of tensile to compressive strengths hence $f_{ctm} = f_{ck} / \chi$.

9.2 Compression-tension-, tension-tension sectors

Here the criteria deduced empirically by Kupfer is the most known one. An elliptical relationship between the two (principal) stresses σ_1 and σ_2 is proposed by Kupfer in case of high transversal compressive stresses, a parabola in case of low ones.

Fig. 13a shows the original figure of Kupfer about the strength development in the compression-tension- and tension-tension sectors. As the vertical axis is made dimensionless with σ_1/β_p, the three concrete grades yield three different curves. With reference to the proposed χ-ratio defined in Chapter 9.1 the dimension of the vertical axis is changed to f_{ct}^* / f_{ct}. Figure 13b shows the curves for the two lower strength concretes. The courses of the two curves can be quite well described with

$$\left(\frac{f_c'^*}{f_c'}\right)^2 + \left(\frac{f_{ct}^*}{f_{ctm}}\right)^2 = 1 \qquad (5)$$

Applying Eq. (5)

$$\left(\frac{f_c'^*}{f_c'}\right)^2 + \left(\frac{\chi \cdot f_{ct}^*}{f_c'}\right)^2 = 1 \qquad (5a)$$

or

$$(f_c'^*)^2 + (\chi \cdot f_{ct}^*)^2 = f_c'^2 \qquad (5b)$$

Ritter tested Ultra High Performance concretes (with short, 2.5% Vol%, 15 mm long steel fibers) having cube (100mm) strength between 170 and 180 N/mm². Figure 13c shows his test results (with very low γ) values.

A comparison of the test results gained on specimens with extreme different strengths let conclude that Eq. (5) describes fairly well the 2D compression-tension behavior of all types of concrete.

Note: The question arises whether at transition from the

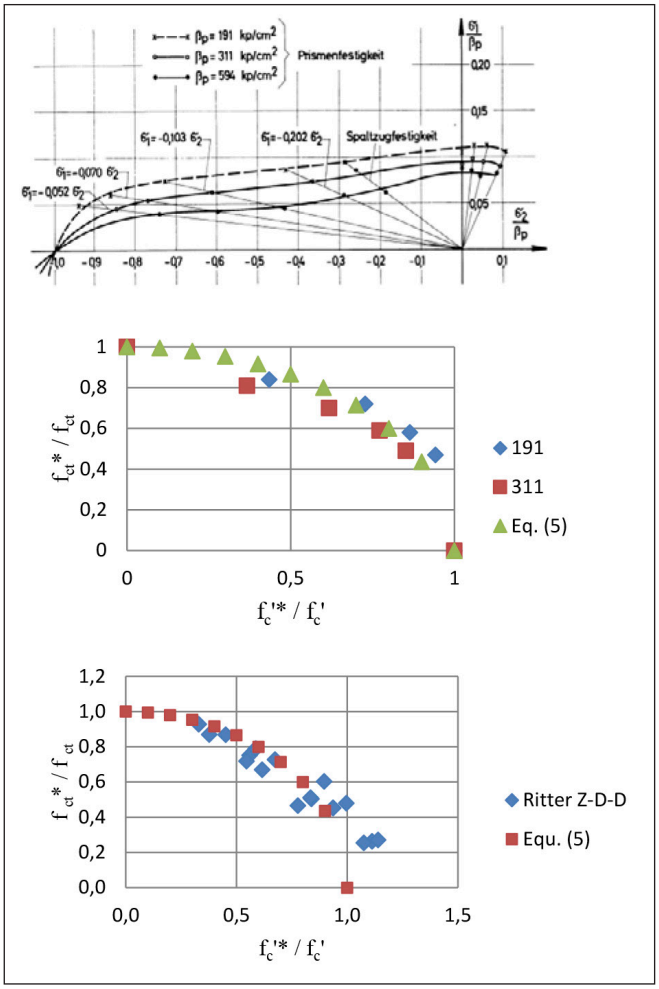

Fig. 13a Mean values of Kupfer's test results in compression-tension and tension-tension sectors (with permission of DAfStb, Berlin)
Fig. 13b New type representation of Kupfer's test results
Fig. 13c New type representation of Ritter's test results in tension-compression sector (γ ~0.01 – 0.075)

sector compression-tension into compression-compression the curve should be smooth or might have a kink. As shown in *Fig. 13a*, Kupfer (1973) suggests a smooth transition. Nevertheless, as the types of failure in these two sectors are fundamentally different, there must be a kink.

In biaxial tension-tension tests the direction with the lower actual tensile strength fails. Here too, the tensile failure patterns pertaining to the two directions are completely independent of each other hence failure occurs in that direction where first the actual tensile strength is reached. "Biaxial tensile strength" does not exist (Lemnitzer et al. (2008)).

9.3 BIAXIAL COMPRESSIVE LOADING

The impending failure of the concrete body in the hydraulic loading equipment is recognized by the fact that, if the amount of hydraulic oil flowing through the valve per unit time is not changed then with less-and-less increasing load increasing deformations occur: the stiffness of the specimen more-and-more decreases. The decrease of the stiffness occurs due to development of more and more microcracks which merge to discrete macrocracks.

The different crack patterns 'produce' different elongated, slim concrete elements which fail at slightly different strengths.

In biaxial compression the discrete macrocracks develop in a prismatic specimen mostly perpendicular to the stress free principal axis and also perpendicular to the axis of the intermediate compressive stress-loading (in case of low transverse loading rate, i.e. $\lambda \leq 0.4$)

In biaxial loading tests the biggest ultimate compressive strength was found around the size $\lambda \approx 0.4$ of the intermediate loading. The explanation can be given on the basis of the measured relative deformations (Kupfer (1973), Speck (2007), Ritter (2014)) as shown in *Fig. 6*.

The course of the intermediate ε_{2u} relative deformations changes its sign around $\lambda \approx 0.4$. In case of $0 \leq \lambda \leq 0.4$ the rate of the transverse (Poisson-type) elongations due to the intermediate loading perpendicular to the axis 1 decreases, i.e. the achievable compressive strength in direction 3 increases. Beyond $\lambda \approx 0.4$ the relative deformations (shortenings) in direction of the intermediate loading increase which more and more contributes to the tensile deformations (development of micro- and discrete macrocracks) perpendicular to the axis 1, therefore the achievable compressive strength, σ_{3u}, decreases again.

10. THE PROPOSED EXTENDED RANKINE FAILURE CRITERIA

After recognizing of the fundamental importance of the principal stresses and that the failure behavior of concrete makes no reference to any friction-type behavior an Extended Rankine Failure Criteria (ERFC) was proposed by the Author (Windisch (2022)).

Rankine (1868) stated in his in 1876 published model that a body fails when any of the three principal stresses exceeds the ultimate tensile strength, regardless of the magnitude of the other principal stresses. It was obvious to extend this criterion to the compressive principal stresses, as well:

- the greatest (> 0) principal stress, σ_1, cannot be greater than the actual tensile strength (its size depends on the size of the σ_2 and σ_3 principal stresses, resp. if at least one of them is compressive stress. (In case of the original Rankine criterion one (fix) tensile strength governed.)
- the triple of the compressive principal stresses $\sigma_3 = \Phi(\sigma_1, \sigma_2)$ cannot be smaller than the actual smallest principal strength, σ_3, which is function of the two other principal stresses,

$$\sigma_3 = \Phi\,(\sigma_1, \sigma_2) \qquad (6)$$

Fig. 14 shows the local ordinates of normalized $-\sigma_3/f_c' = \Phi\,(\sigma_1/f_c', \sigma_2/f_c')$ function as deduced from the bi- and triaxial tests measured by Speck (2007) on $f_c' = 72$ N/mm² test specimens.

Fig. 15 presents the Ultimate Strength Surface, USS, in another form: the abscissa is $\gamma = \sigma_1 / \sigma_3$, the ordinate is $\lambda = \sigma_2 / \sigma_3$. The USS increases monotonic in the γ-direction, whereas increases up to $\lambda = 0.4 \sim 0.6$ then decreases moderately.

Having determined the relevant failure causing principal stresses the corresponding normal- and shear stress components in the global coordinate system can be determined using Mohr-circles or the tensor calculus. Note: the global shear stress components calculated from the failure causing principal stresses refer by no means to any shear failure!

11. CALIBRATION OF THE STRENGTH FAILURE CRITERIA IN MC 2010

Following the proposals of Ottosen (1977), MC 2010 (2013) uses four strength values for calibration: the uniaxial tensile strength, the uniaxial compressive strength (point on the compressive meridian), the biaxial compressive strength (point on the tensile meridian), and a triaxial compressive strength at one point on the compressive meridian ($\sigma_1 = \sigma_2 > \sigma_3$) described by the octahedron stresses. The red arrows in *Fig. 14* mark these strength values revealing that they are not suitable for describing the USS.

Note: Kupfer's biaxial strength curves reveal that even the uni- and biaxial strength values are absolute not representative for the course. Also the strength values along the compressive meridian are of very limited informative value. The maximum strength increase could be anticipated with $\gamma = \lambda = 0.5 \sim 0.6$. With her very advanced test equipment Speck achieved $\gamma = \lambda = 0.15$ only. The double-curved surface of the USS does not allow any reliable extrapolation relying on $\gamma = \lambda = 0$ and $\gamma = \lambda = 0.15$ values. Here further tests are necessary.

Fig. 14: Local ordinates of normalized $-\sigma_3/f_c' = \Phi(\sigma_1/f_c', \sigma_2/f_c')$ function as deduced from the bi- and triaxial tests measured by Speck (2007) on $f_c' = 72$ N/mm² test specimens

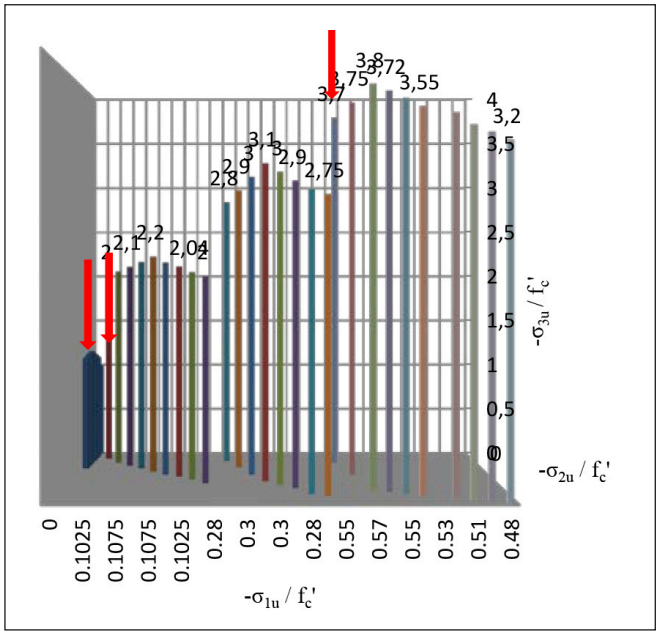

Fig. 15: The Ultimate Strength Surface compiled from the data measured by Speck (2007)

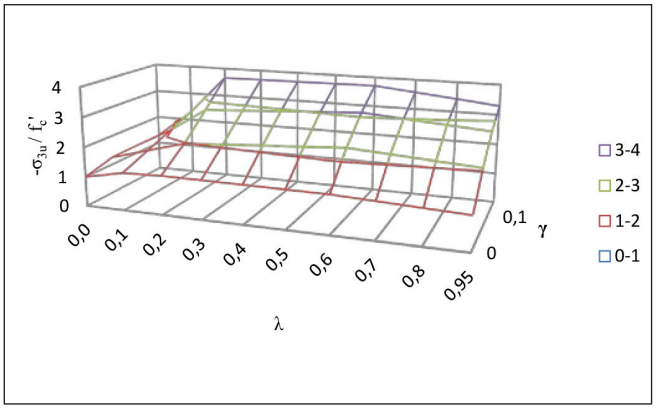

12. CONCLUSIONS

The development of the failure models corresponds to the possibilities of the testing equipment and follows the achievements of the numerical calculation methods.

All experiments, also the uniaxial ones, are/must be essentially considered as tri-axial. Concrete knows/obeys principal stresses only. Concrete does not have any shear strength. Shear stress is the consequence of our hugging to the global coordinate system only.

Based on the principal stresses and their relationship i.e. the loading paths as independent variables, a new, transparent (and physically really sound) form of representation of the failure surface (USS) showing the strength increase due to bi- and triaxial loading is presented. This paper focus on the increasing branch of the stress-strain curve up to the peak stress only.

Any target triaxial ultimate strength can be reached following the loading path only: with a biaxial loading an increase of maximum 10-20% can be achieved only. Beyond this level loading/strain restriction in the third direction is necessary to let increase the maximum compressive strength in the 'main/leading' direction. Simplified relative strength increasing factors for concrete classes ≤ C100 are presented.

Problems and difficulties at deformation measurements are discussed. At evaluation of the strength- and strain values the impact of the loading equipment and the measuring methods must be considered: the elongations refer to development of pronounced discrete cracks, nevertheless remarkable compressive loading is transmitted perpendicular to this (these) cracks. Further systematic tests are necessary.

Reference is made that due to intense development of discrete cracks rules of continuum mechanics shall be applied with reservation. As failure modes the tensile failure and compression failure after splitting are identified. The 'shear' failure occurs due to deviations in the loading system only. A simple stress failure criterion is proposed for biaxial compression-tension loading. The tensile strengths in the three principal directions are independent from each other.

Extended Rankine Failure Criteria is presented: i) the greatest (> 0) principal stress, σ_1, cannot be greater than the actual tensile strength, ii) the triple of the compressive principal stresses $\sigma_3 = \Phi(\sigma_1, \sigma_2)$ cannot be smaller than the actual smallest principal strength, σ_3, which is function of the two other principal stresses. The calibration of the strength failure criteria in MC2010 is discussed.

Further systematic tests are needed before more reliable failure criteria could be formulated for multiaxial loaded concrete.

13. REFERENCES

Comité Euro-international du Béton, (1983) Bulletin d'information N° 156: Concrete under multiaxial states of stress. "Constitutive equations for practical design ». Contribution à la 23e Session plenière du C.E.B. Prague – Octobre 1983, Juin 1983, p. 149.

Drucker, DC, Prager, W., (1952), "Soil Mechanics and Plasticity Analysis of Limit Design". Quarterly of Applied Mathematics, 1952; Vol. 10, No. 2, 157-165. https://doi.org/10.1090/qam/48291

fib Model Code for Concrete Structures 2010 (MC2010), (2013), Fédération international du béton, Oct. 2013, Ernst & Sohn, Berlin, p. 434. https://doi.org/10.1002/9783433604090

Hillerborg, A., Modéer, M., Peterson, P.E. (1976), "Analysis of crack formation and crack growth in concrete by means of fracture mechanics and finite elements", Cement and Concrete Research, 1976; Vol. 6, 773-782. https://doi.org/10.1016/0008-8846(76)90007-7

Hilsdorf, H., (1965) Versuchstechnische Probleme beim Studium der zweiachsigen Festigkeit des Betons. Sonderdruck, 1965; Heft 173 der Schriftenreihe des Deutschen Ausschusses für Stahlbeton.

Kármán von, Th., (1910), "What determines the stress-strain behavior of materials?" (In Hungarian: Mitől függ az anyag igénybevétele?), Journal of the Society of Hungarian Engineers and Architects, 1910; Vol. XLIV, No. X, 212–226

Kupfer, H. (1973), „Das Verhalten des Betons unter mehrachsiger Kurzzeitbelastung unter besonderer Berücksichtigung der zweiachsigen Beanspruchung", Deutscher Ausschuss für Stahlbeton, 1973; Heft 229, Ernst und Sohn, Berlin, p. 105.

Newman, K, Siqvaldason, OT. (1965), "Testing machine and specimen characteristics and their effect on the mode of deformation, failure and strength of materials". Proc. Inst. Mech. Engrs., 1965-66, Vol. 180, part 3A, pp. 399-410. https://doi.org/10.1243/PIME_CONF_1965_180_048_02

Lemnitzer, L, Eckfeldt, L, Lindorf, A, Curbach, M., (2008), "Biaxial strength of concrete – answers from statistics in Tailor Made Concrete Structures" – Walraven & Stoelhorst (eds). 2008; ISBN 978-0-415-47535-8, pp. 1101-1002.

Ottosen, NS., (1977), "A Failure Criterion for Concrete". Journal of Engineering Mechanics, Div. ASCE, 1977; Vol 103, EM4. https://doi.org/10.1061/JMCEA3.0002248

Rankine, WJM, (1868) A Manual of Applied Mechanics. 1868; London

Ritter, R. (2014), „Verformungsverhalten und Grenzflächen von Ultrahochleitsungsbeton unter mehraxialer Beanspruchung", Dissertation, 2014; TU Dresden, p. 280.

Speck, K., (2007), „Beton unter mehraxialer Beanspruchung. Ein Materialgesetz für Hochleistungsbetone unter Kurzzeitbelastung, Concrete under multiaxial loading conditions. A Constitutive Model for Short-Time Loading of High Performance Concretes". Dissertation, 2007; TU Dresden, p. 224.

Stroeven, P., (1973), "Some aspects of the micromechanics of concrete". Dissertation, 1973; Delft.

Van Mier, JGM. (1984), "Strain-Softening of Concrete under Multiaxial Loading Conditions", Dissertation, TH Eindhoven, 1984; p. 363.

Windisch A, (2021).." The tensile strength: the most fundamental mechanical characteristics of concrete". Concrete Structures, 2021; Vol. 22, pp. 1-4. https://doi.org/10.32970/CS.2021.1.1

Windisch, A., (2022), "Extended Rankine Failure Criteria for Concrete". Concrete Structures, 2022; Vol. 23, pp. 4-10, https://doi.org/10.32970/CS.2022.1.2

NOTATIONS

I_1	first invariant of the stress tensor;
J_2, J_{2c}, J_3, J_{3c}	second and third invariants of the stress deviators
f	yield function (MC2010)
f_c'	concrete compressive strength
f_c*, f_{ct}*	compressive and tensile stresses in 2D and/or 3D loading
f_{ck}	characteristic concrete compressive strength
f_{cm}, f_{ctm}	mean compressive and tensile strength, resp.
f_{c2cm}	biaxial compressive strength
α, β, c_1 and c_2	material parameters (Ottosen)
β	prism strength (Kupfer)
ε_{1u}, ε_{2u}, ε_{3u}	ultimate strains in principal directions 1 to 3
$\gamma = \sigma_1 / \sigma_3$	loading parameter
ε_i	strain measured in test
ε_{iu}	ultimate strain measured in test in i^{th} principal direction
$\lambda = \sigma_2 / \sigma_3$	loading parameter
Φ	relative ultimate strength as function of the loading path
$\chi = f_{ck}/f_{ctm}$	ratio of characteristic concrete compressive strength to mean tensile strength
σ_1, σ_2, σ_3	principal stresses ($\sigma_1 \geq \sigma_2 \geq \sigma_3$)
σ_{3u}	ultimate strength measured in test
σ_{com}	hydrostatic normal stress
τ_{com}	octahedral shear stress
[γ, λ, 1]	stress-loading path
[1, 1, σ_{c3u}]	ultimate hydrostatic normal strength (cap value)

Andor Windisch PhD, Prof. h.c. retired as Technical Director of DYWIDAG-Systems International in Munich, Germany. He made his MSc and PhD at Technical University of Budapest, Hungary, where he served 18 years and is now Honorary Professor. Since 1970 he is member of different commissions of FIP, CEB, *fib* and ACI. He is author of more than 190 technical papers. Andor.Windisch@web.de